Microsystem Technologies (2020) 26:1625–1635
https://doi.org/10.1007/s00542-019-04703-w

TECHNICAL PAPER

Analysis of a novel RF MEMS switch using different meander techniques

K. Girija Sravani[1,2] · Koushik Guha[1] · K. Srinivasa Rao[2]

Received: 16 May 2019 / Accepted: 23 November 2019 / Published online: 2 December 2019
© Springer-Verlag GmbH Germany, part of Springer Nature 2019

Abstract

In this paper, two types of RF MEMS switches namely step structure and Normal beam structure are designed and analyzed using different meander techniques. Three techniques namely plus, zigzag and three-square meander were used to lower the pull-in voltage. The actuating beam is designed with the rectangular perforations affects the performance of a switch by lowering the pull-in voltage, switching speed and results in better isolation. In this paper a comparative analysis is done for all three meander techniques with and without perforations on the beam. Total six structures have been designed with the combination three meanders and two different beam structures. The proposed stepdown structure exhibits high performance characteristics with a very low pull-in voltage of 1.2 V having an airgap of 0.8 µm between the actuation electrodes. The gold is used as beam material and HfO_2 as the dielectric material such that the upstate and downstate capacitance is seen as 1.02 fF and 49 fF. The FEM analysis is done to calculate the spring constant and thereby the pull-in voltage and behavior of the switch is studied with various parameters. The switch with a step structure and three-square meander configuration has shown best performance of all by requiring a pull-in voltage of 1.2 V and lower switching time of 0.2 µs. The proposed switch also exhibits good RF performance characteristics with an insertion loss below − 0.07 dB and return loss below − 60 dB over the frequency range of 1–40 GHz. At 28 GHz a high isolation of − 68 dB is exhibited.

1 Introduction

In the recent years, MEMS technology had gained tremendous attention from both industry and academia. As the miniaturization is the key feature, MEMS technology is used everywhere in modern day electronics (Rebeiz 2003). MEMS devices tend to show a high linearity and low power consumption. Due to its batch fabrication processes bulk manufacturing can be done bringing down the fabrication costs. It has that unique quality of creating a platform on which the electrical and mechanical components can be monolithically integrated (Rao and Sravani 2018; Sravani and Rao 2018). The MEMS devices had another major advantage because of their ability to operate at wide range of frequencies. In the recent years telecommunication industries are adopting this technology at a rapid pace. Ultra-wide frequency range makes these devices better when compared with the traditional FET and PIN diode in many applications (Molaei and Ganji 2017). When compared to their solid-state counterparts the MEMS switches consume relatively less power, maintains high linearity and reliability. Due to this, they are replacing the traditional FET switches and PIN diodes (He et al. 2011). There development is much needed as they can be used in a wide number of applications such as switching elements in reconfigurable antennas, satellites, mobile devices and other short-range applications (Katehi et al. 2002). The MEMS switches also include different operating principles i.e., the series switches and the shunt switches. The beam of the switch is also implemented with two different configurations such as fixed–fixed and cantilever structures.

Different actuation techniques are available to actuate a switch. The electrostatic actuation is preferred (Öjefors 2004) among them. So, it is required to do the optimizations to lower the pull-in voltage required to actuate the switch. In this paper the designed capacitive shunt switch is subjected to different optimizations. The structure is

✉ K. Girija Sravani
kondavitee.sravani03@gmail.com

1 Department of Electronics and Communication Engineering, National MEMS Designing Center, National Institute of Technology, Silchar, Assam, India

2 Department of Electronics and Communication Engineering, MEMS Research Center, KL University, Green Fields, Vaddeswaram, Guntur 522502, India

simulated at different configurations i.e., by using different meander techniques namely square shaped, zigzag and plus shaped meanders. This analysis is done with and without the perforations on the beam. As the air gap between the beam and the dielectric layer is also one of the main aspects to consider, a novel step structure is also implemented and analyzed for the designed switch. This step-down structure reduces the airgap thereby reduces the switching time and actuation voltage required. By comparing all the simulated values, we found that stepdown structure with uniform three square meander offers better performance requiring a low pull-in voltage of 1.2 V and exhibiting a high isolation of − 61 dB at 28 GHz. This structure also had a low insertion loss of − 0.7 dB over the frequency of 40 GHz.

2 Proposed switch materials

MEMS capacitive shunt switches are designed over the transmission lines to bypass the propagating signal by offering low impedance across it. Fixed–fixed type switches are most common shunt type of switches used in RF applications operating over 10 GHz (Papapolymerou and Drayton 1998). The schematic of the proposed switch structures as shown in the Fig. 1 consists of high dielectric substrate having 200 µm thickness made up of silicon. The insulating layer of 1 µm thickness is deposited on the substrate to avoid leakage currents. The CPW transmission line of 35/60/35 of thickness 1 µm is considered over the insulating layer for the propagation of RF signal. A thin dielectric layer of 0.5 µm thickness is deposited over the signal line of CPW to create a capacitive path for the propagating signal. Two biasing electrodes are considered in between the signal line and ground planes which are present below central beam with a gap of 1 µm. Electrostatic forces are generated when a potential difference is applied between the centre beam and biasing electrodes for the actuation of switch Using these biasing pads RF input signal is isolated with the actuation voltage during the operation of switch. Anchors are placed on the two ground planes such that the central beam is suspended between the anchors over the CPW. The central beam of 1 µm thickness consists of the capacitive beam present at the centre and actuation beam presented on either side of the capacitive beam as shown in the Fig. 2.

Two types of switches are proposed according to the structure of the central beam switch A: normal beam structured switch having capacitive and actuation beams are in same horizontal plane as shown in Fig. 3a and switch B: named as step structured switch having the capacitive beam below the actuation beams connected with the step contact as shown in the Fig. 3b.

Normal fixed–fixed switches possess high pull-in voltage due to large stiffness of the central beam (Roark and Young 1989). Hence to reduce pull-in voltage meandering technique (Marcelli et al. 2010) can be implemented. Three types of meander techniques were mainly implemented for the proposed structures. Using the meanders instead of a solid central beam. Different meanders used are rectangular, square and cylindrical shaped meanders. The below Fig. 4 represents the schematic of a 3 square meander and these dimensions are given in the Table 1.

The Fig. 5 represents the schematic of a plus shaped meander with the dimensions explained in Table 2.

The Fig. 6 represents the schematic of Zigzag meanders which comes under the non-uniform meander type and the dimension of the zig-zag meander is given the Table 3.

Material selection is one of the most important practice to consider while designing a device. Gold is chosen as a material for the beam, biasing electrodes, CPW, meanders and step contacts due its high conductivity (Kumar et al. 2018) than any other materials. Silicon is the suitable material for the substrate having high young's modulus, possibility for monolithic integration and high electrical resistivity of 6.4×10^2 Ω-m (Ramli and Sidek 2012). SiO_2 is taken as the suitable material for the insulating layer having very high electrical and temperature resistivity and is highly used to avoid leakage currents and insertion losses (Chakraborty et al. 2014). HfO_2 is chosen as the dielectric

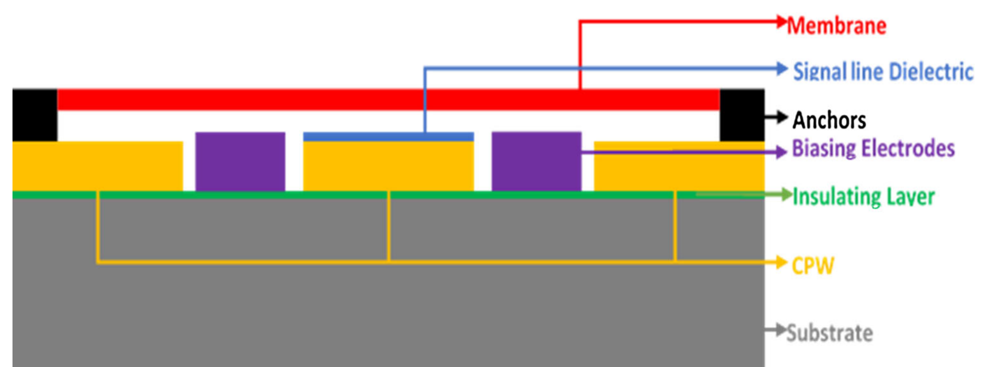

Fig. 1 Schematic view of fixed–fixed RF MEMS switch

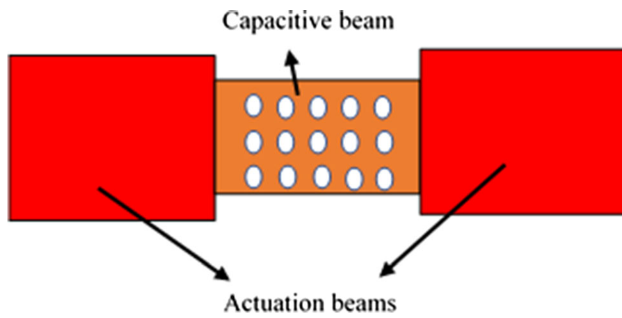

Fig. 2 Top view of beam with perforations

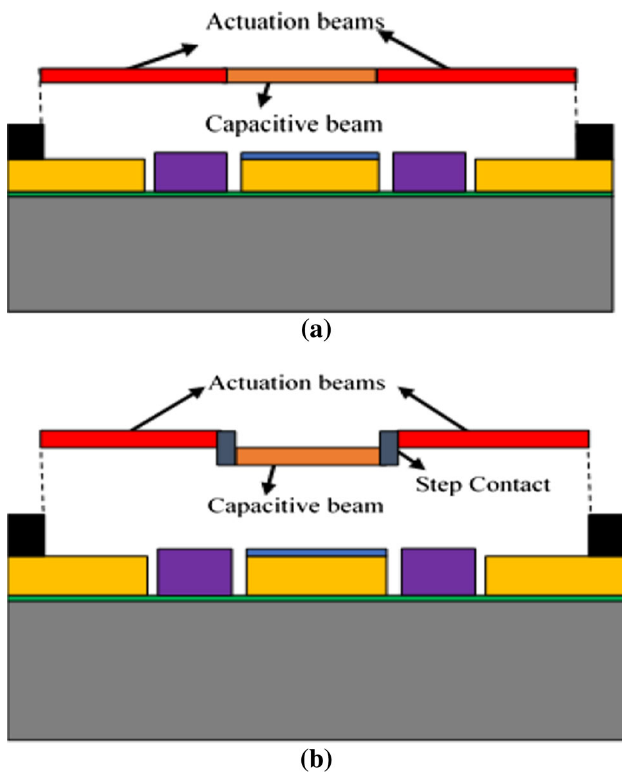

Fig. 3 **a** Switch A: normal beam structured switch. **b** Switch B: step down structured switch

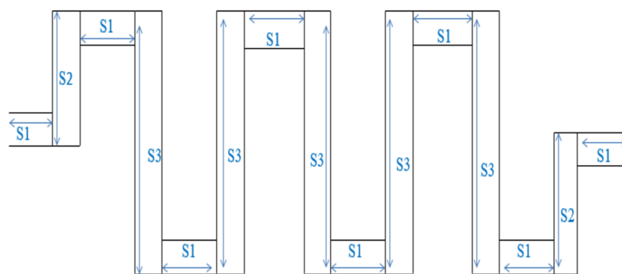

Fig. 4 Serpentine shaped meander

layer because of large band-gap, E_g = 5.6–5.8 eV, high dielectric permittivity κ = 16–25 and high thermal stability (Angira and Rangra 2015). The perforations in a beam

Table 1 Dimensions of the individual blocks in square shaped meander

Spring blocks	Length (μm)	Width (μm)	Height (μm)
S1	5	1	1
S2	1	20.5	1
S3	40	40	1

μm Micrometers

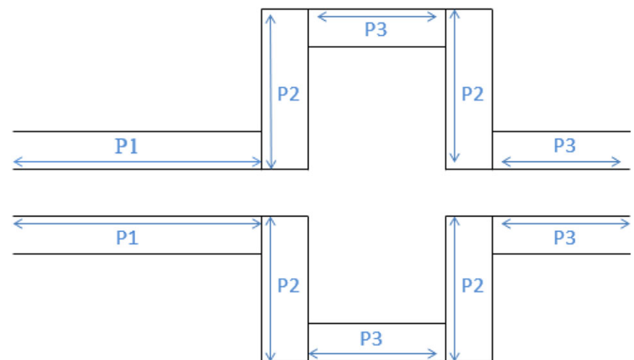

Fig. 5 Plus shaped meander

Table 2 Dimensions of the blocks in the plus shaped meander

Spring blocks	Length (μm)	Width (μm)	Height (μm)
P1	25	1	1
P2	1	15	1
P3	10	1	1

μm Micrometers

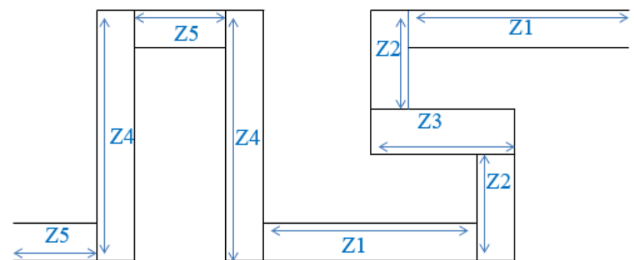

Fig. 6 Zigzag shaped meanders

plays an important role in reducing the mass of the beam and the drag experienced by the beam. Also, it makes the beam more flexible. The beam is studied when rectangular perforations of dimensions 4 μm × 2 μm × 1 μm are made on the central beam. By comparing the obtained simulation results we observed that rectangular shaped perforations resulted in better efficiency of the switch. The dimensions of the different shapes of perforations are given in Table 2. By proposing three type of meanders and two

Table 3 Dimensions of the blocks in the zigzag meander

Spring constant	Length (μm)	Width (μm)	Height (μm)
Z1	22	1	1
Z2	1	7	1
Z3	18	1	1
Z4	1	15	1
Z5	10	1	1

The dimensions of the proposed switches illustrated in the Table 4

types of structures totally six different types of RF MEMS switches have been proposed.

3 Results and discussions

3.1 Mechanical analysis

3.1.1 Spring constant

The meanders introduced in the switches provides the necessary spring constant or stiffness to hold the centre beam which is suspended over CPW. This meandering technique used to obtain the low spring constant when compared to the fixed–fixed beam type switches. The spring constant of the total meander can be obtained by calculating the stiffness of each individual beam which are in series combination. Generally, the stiffness of each individual beam can be calculated with the Eq. (1) (Jaspreet et al. 2014)

$$K = \frac{Ywt^3}{l^3} \quad (1)$$

where K is the stiffness, w is the width, t is the thickness and l is the length of each individual blocks in the meanders. The inverse of the spring constant of each meander can be obtained by the summation of inverse of each block stiffness present in each meander. Hence the spring constants of different meander are given by the equations (Guha et al. 2016)

$$\frac{1}{s} = \frac{8}{s_1} + \frac{2}{s_2} + \frac{5}{s_3} \quad \text{for serpentine meander} \quad (2)$$

$$\frac{1}{p} = \frac{1}{p_1} + \frac{2}{p_2} + \frac{2}{p_3} \quad \text{for serpentine meander} \quad (3)$$

$$\frac{1}{z} = \frac{2}{z_1} + \frac{2}{z_2} + \frac{1}{z_3} + \frac{2}{z_4} + \frac{2}{z_5} \quad \text{for serpentine meander} \quad (4)$$

where s, p and z are the spring constant of single meanders of serpentine, plus and zig-zag spring structures. Three types of switches can be designed using proposed three meanders and the switches contains centre membrane supported by two meanders in serpentine meandered switch, four meanders by the plus meandered switch and two meanders in zig-zag meandered switch. Hence the total spring constant of three types of switches are

$$K_s = 2s \quad (5)$$

$$K_p = 4p \quad (6)$$

$$K_z = 2z \quad (7)$$

where K_s, K_p and K_z are the total spring constants of the proposed serpentine, plus and zig-zag meandering switches and analytically these are obtained as 0.46, 1.2, 4.6 respectively. These analytical calculations of the spring constant is validated by simulating the proposed switches in FEM tool. The simulation is carried according to the newton's mass-spring-damper system which postulates that the displacement of the mass is directly proportional to the applied force.

$$F \propto X \quad (8)$$

Therefore,

$$K = \frac{F}{X} \quad (9)$$

where K is the spring constant, x is the displacement and F is the applied force. Hence the spring constant of the switch is the ratio of applied force and displacement of the mass. Here the mass resembles total mass of the centre beam.

The simulated spring constant of each type of meander is obtained by applying a sweep of force on the beam and displacement of the beam is observed and are substituted in the Eq. (9). The Figs. 7, 8 and 9 describes the FEM simulations of displacement of the centre beam suspended by the three meanders. The ratio of force to the displacement along Z component gives the required spring constant

3.1.2 Impact of acceleration due to gravity

The deflection of the switch membrane due to acceleration is given by (Bachman et al. 2012)

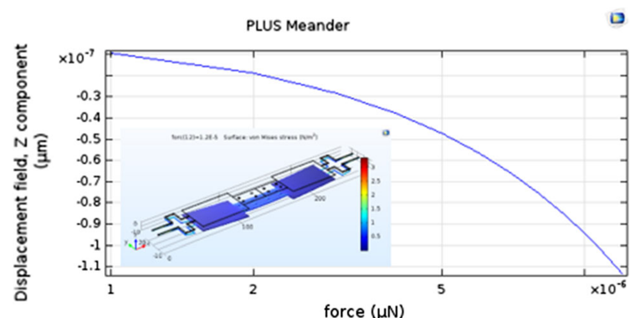

Fig. 7 Force vs displacement of plus meander

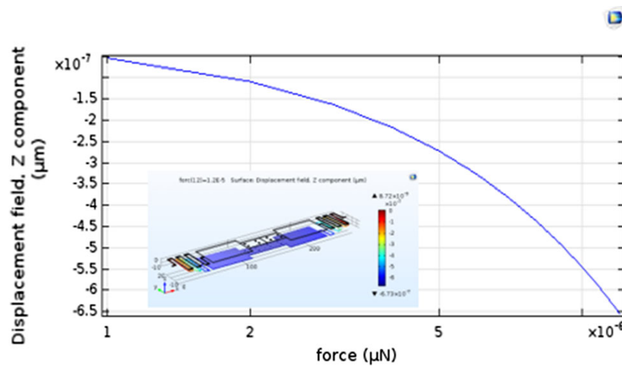

Fig. 8 Force vs displacement of serpentine meander

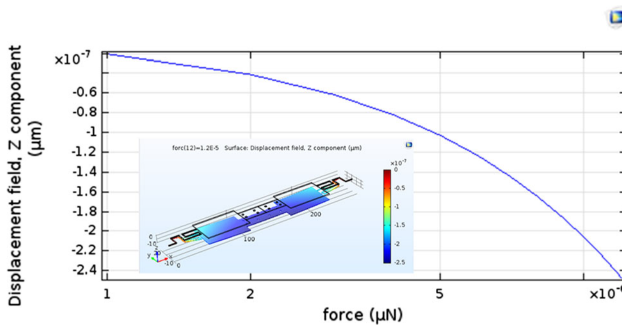

Fig. 9 Force vs displacement of zig-zag meander

$$\Delta x = \frac{F}{K} = \frac{mg}{K} = \frac{(lwt)\rho g}{K} \quad (10)$$

where Δx is the deflection of beam, F is the force acting on the beam due to acceleration due to gravity, g is the acceleration due to gravity, ρ is the density of the beam material, *l*, w and t are the length, breadth and thickness of the beams and K is the spring constant of the meanders (Tables 4, 5, 6).

Generally, the MEMS switches are not sensitive to the acceleration due to gravity. An acceleration of g = 9.8 m/s^2 exerts a force of 1.13 nN on the beam having mass 1.15×10^{-10} kg and the beams deflects vertically downwards for gold material beam with a spring constant of meanders. The deflection is presented in the Table 7.

For a gap of 1 µm, a negligible displacement is observed in both analytical and simulation results as shown in Figs. 10, 11 and 12. Hence the proposed switches are not sensitive to acceleration forces because the displacements are very small.

3.1.3 Reliability of the switch

The reliability of the switches depends on ability to restore its original position i.e., upstate condition. The meanders are responsible to provide these restoring forces against the electrostatic actuation. Stiction and air damping reduces

Table 4 Dimensions of the blocks in the zigzag meander

Component	Length (µm)	Width (µm)	Height (µm)
Substrate	240	60	200
Insulating layer	240	60	1
Dielectric Layer	60	50	0.5
Anchors	3	60	1
Biasing electrodes	30	40	1
Actuation Beam	40	40	1
Capacitive Beam	60	20	1
Step contact	0.2	20	0.2

µm Micrometers

Table 5 Spring constant of proposed meanders

Meander type	Spring constant (N/m)	
	Analytical	Simulated
Serpentine	0.46	0.54
Plus	1.2	1.05
Zig-zag	4.6	4.8

N/m Newton per meter

Table 6 Dimensions for the perforations used in study

Meander type	Deflection by acceleration due to gravity	
	Analytical	Simulated
Serpentine	2.4 nm	2.24 nm
Plus	87 pm	75.8 pm
Zig-zag	0.18 nm	0.191 nm

Table 7 Pull-in voltage of normal beam switches

Meander type	Pull-in voltage (V)	
	Analytical	Simulated
Serpentine	1.8	2.1
Plus	9.5	10.2
Zig-zag	6.5	6.9

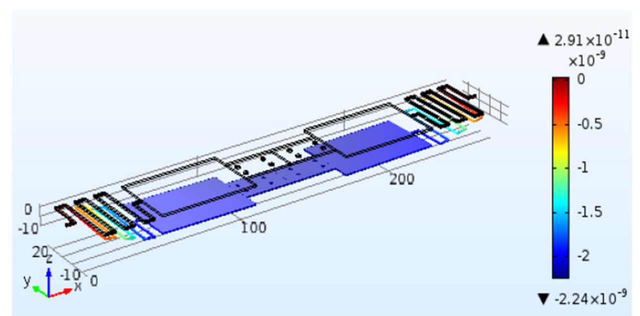

Fig. 10 Displacement of serpentine meander due to acceleration due to gravity

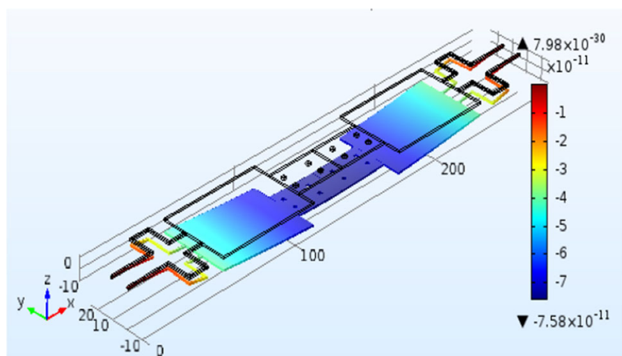

Fig. 11 Displacement of plus meander due to acceleration due to gravity

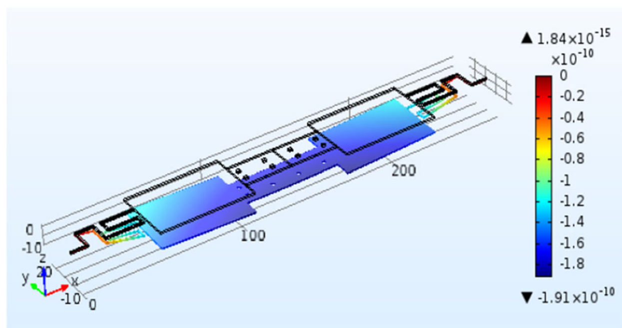

Fig. 12 Displacement of zig-zag meander due to acceleration due to gravity

this restoring force. Hence perforations are created on the capacitive beam such that the stiction between the beam and dielectric layer is nullified. The air damping of the switch membrane has to be reduced and is given as (Bachman et al. 2012)

$$b = \frac{3}{2}\frac{\mu A^2}{g_0^3} \quad (11)$$

where b is the coefficient of damping, μ is air viscosity (1.885 × 10^{-5} Pa), g_0 is the air gap (1 μm for normal beam and 0.8 μm for step down switch) and A is the overlapping. Thus, the damping coefficient obtained is 2.15 × 10^{-6} for normal switch and 2.69 × 10^{-6} for step down switch. The low damping ratio of the switches made them reliable for large number of duty cycles.

3.2 Mechanical analysis

3.2.1 Pull-in voltage

The proposed six switches have designed and simulated using FEM tool. The switch is simulated by applying the voltage difference between the biasing pads and actuation beams. This voltage difference gives rise to the electrostatic forces between them and pulls down the centre beam.

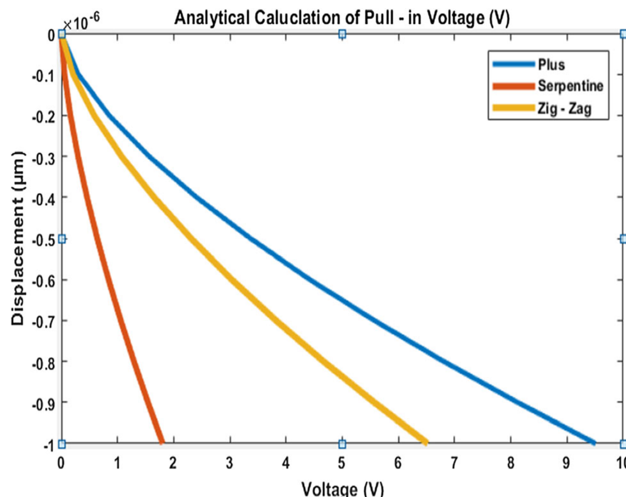

Fig. 13 Voltage vs displacement for normal beam structure

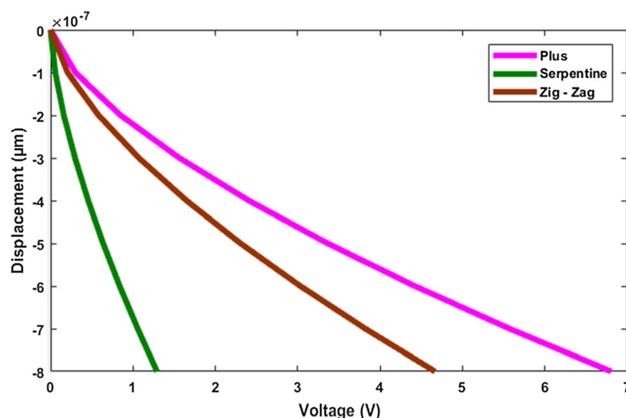

Fig. 14 Voltage vs displacement for step structure switches

The capacitance will develop between the centre beam and signal line due to dielectric layer present between them. The voltage at which the beam touches dielectric layer is called pull-in voltage and switch breakdown occurs.

From the Figs. 13 and 14, It is observed that in step down structure the gap between the capacitive beam and signal line is maintained at 0.8 μm hence the beam

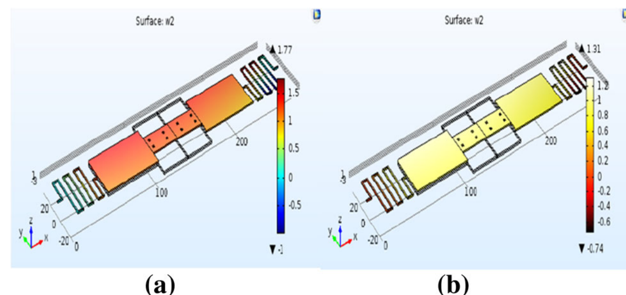

(a) **(b)**

Fig. 15 **a** Displacement of zig-zag meander type normal beam switch. **b** Displacement of zig-zag meander type step down beam switch

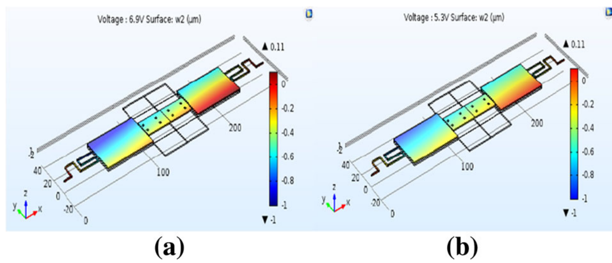

(a) (b)

Fig. 16 a Displacement of zig-zag meander type normal beam switch. b Displacement of zig-zag meander type step down beam switch

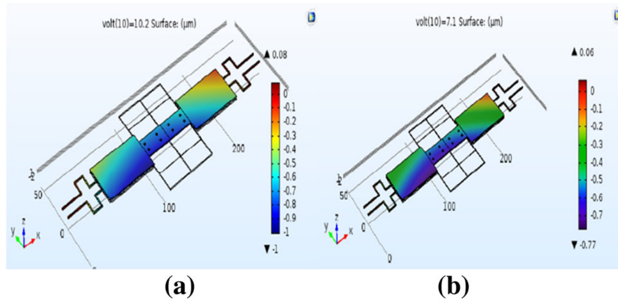
(a) (b)

Fig. 17 a Displacement of plus meander type normal beam switch. b Displacement of plus meander type step down beam switch

displaces with a low pull-in voltages than the normal beam switches. The serpentine step structure switch has very low pull-in voltage of 1.4 V and is good practice to develop these kinds of switches for low power applications.

The Figs. 15, 16 and 17 depicts the simulation results normal switch and step structure switch designed with three types of meanders. The simulation and analytical results on pull-in voltage have discussed in the Tables 8 and 9.

It is observed that among all the switches the pull-in voltage of serpentine step structure switch has very low pull-in voltage of 1.4 V than the other type of switches. Hence the step structured serpentine structured switch is efficiently used in low power applications.

the hysteresis verification is done by simulating the serpentine step structure switch using FEM tool and observed the transition between the ON–OFF states of serpentine step structure switch when a range of discrete voltages are applied. When switch is actuated the centre

Table 8 Pull-in voltage of step switches

Meander type	Pull-in voltage (V)	
	Analytical	Simulated
Serpentine	1.2	1.4
Plus	6.8	7.1
Zig-zag	4.6	5.3

Table 9 Comparison of capacitance values of serpentine step structure switch

Serpentine step switch	Capacitance (fF)	
	Analytical	Simulated
C_{off}	1.23	1.02
C_{on}	53	49

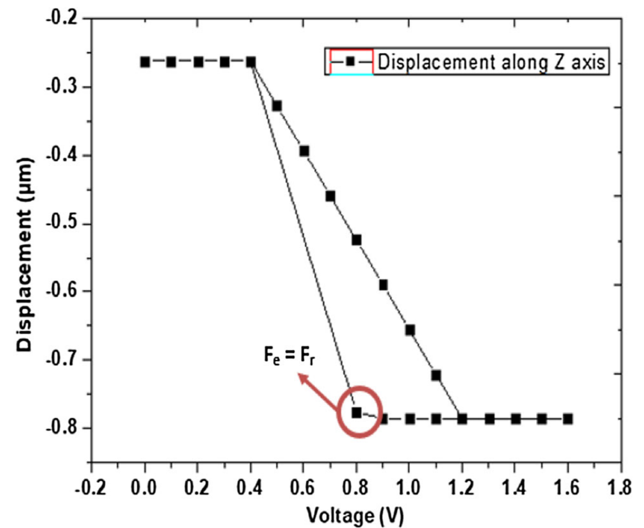

Fig. 18 Hysteresis of serpentine step structure switch

membrane deflects due to electrostatic forces and touches the dielectric at the pull-in voltage and when the actuation voltage gradually decreased then the switch is released due to restoring forces of meanders (Sharma et al. 2015). The switch starts regaining its original position when the restoring forces dominates the electrostatic forces. The hysteresis cycle is shown in Fig. 18 and obtained pull-in and release voltages are respectively 1.2 and 0.8 V.

3.2.2 Cross-sensitivity analysis

The proposed MEMS switches must deflect vertically downwards only, any movement or deflection in other direction results in very low capacitance value as the overlapping area decreases and it effects working mechanism of the switch. Hence the switches must be negligible displacement in X and Y axis.

It is observed that the switches have very less deflection towards Y axis as shown in the Figs. 18, 19 and 20 when compared to the displacement of the along Z direction.

3.2.3 Capacitance ratio

The RF response of a shunt capacitive switch having a fixed–fixed beam depends on the capacitance ratio of the switch. The capacitance ratio is given by the ratio of down-

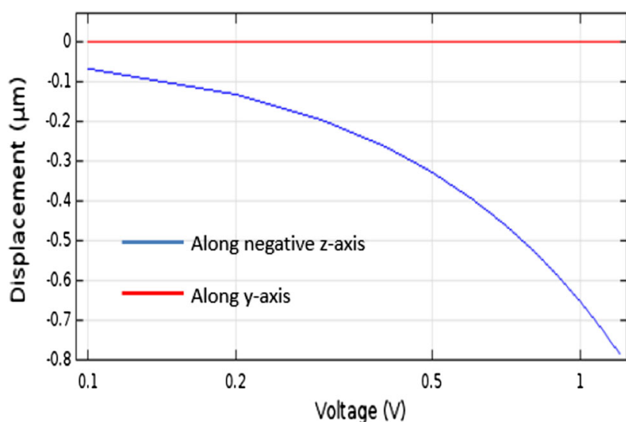

Fig. 19 Displacement of serpentine step structure switch along Z and Y axis

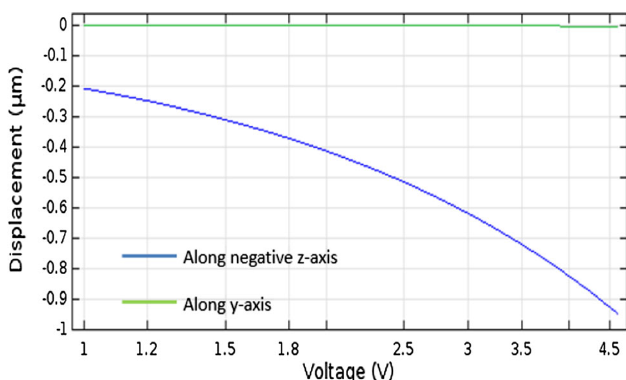

Fig. 20 Displacement of zig-zag meander structure switch along Z and Y axis

state capacitance (C_{down}) to the Up-state capacitance (C_{up}). The CON or CUP is the upstate capacitance seen when the switch is in the on state. It is given by the Eq. (12) (Balaraman et al. 2012)

$$C_{ON} = \frac{\varepsilon_0 ab}{g_0 + \frac{t_d}{\varepsilon_r}} \tag{12}$$

where a is the length of the capacitive beam, b is the width of the capacitive beam, ε_0 s the permittivity of the free space, ε_r is the relative permittivity of dielectric material, g_0 is air gap, t_d is the oxide layer thickness. The upstate capacitance changes as the material changes, because relative permittivity is not same for every material. It also changes with variation of airgap. In these proposed switches the capacitive beam dimensions are identical hence same on-state and off-state capacitances occur. The serpentine switch is simulated and presented to obtain the capacitance values,

By observing the above it can be said the upstate capacitance value decreases as the airgap between the beam and the dielectric layer increases.

C_{off} is the down state capacitance. It can be measured by using the equation

$$C_{off} = \frac{\varepsilon_0 \varepsilon_r ab}{t_d} \tag{13}$$

The Coff is 49.1fF and C_{on} of 1.02fF is observed by simulations. The capacitance ratio can be calculated by using Eq. (14) (Fedder 1994)

$$C_{ratio} = \left(\frac{C_{off}}{C_{ON}}\right) = \frac{\frac{\varepsilon_0 \varepsilon_r ab}{t_d}}{\frac{\varepsilon_0 ab}{g_0 + \frac{t_d}{\varepsilon_r}}} \tag{14}$$

The capacitance ratio can also be described as the figure of merit and it is obtained from the Eq. (13) is 48. The analytical and simulated capacitance values are presented on the Table 10.

3.3 Time dependent analysis

3.3.1 Switching time

The switching time of the switches can be obtaining by the Eq. 15 and is defined as the deflection of the beam from upstate to downstate. It is strongly depending on the actuation voltage and resonant frequency and is obtained from the Eq. (12) (Lee et al. 2015)

$$T_s = \frac{3.67 V_p}{V_s \omega_0} \tag{15}$$

The switching time of the proposed step structure switches are calculated with the Eq. (15) and presented in the Table 10.

From the Figs. 20, 21 and 22, it is observed that transition of switches from ON state to OFF state requires nearly 0.2 μs. Among these the plus and zig-zag meanders have low switching time than the serpentine structure. The values of switching time presented in the Table 10 gives fast switching time during actuation of switches.

3.4 RF performance analysis

The dc voltage is applied to the beam and the dielectric layer acts as the ground. The electrostatic force is

Table 10 Switching time

Meander type	Switching time (μm)	
	Analytical	Simulated
Serpentine	0.23	0.2
Plus	0.18	0.16
Zig-zag	0.17	0.16

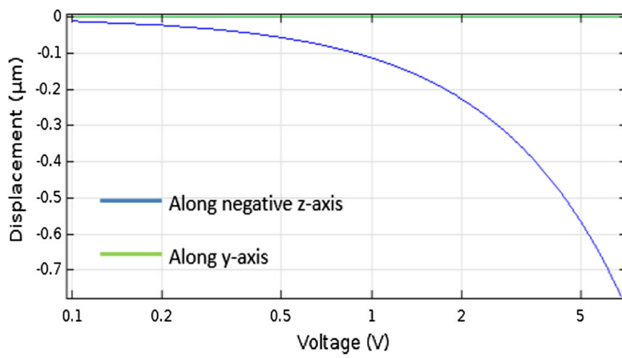

Fig. 21 Displacement of plus meander structure switch along Z and Y axis

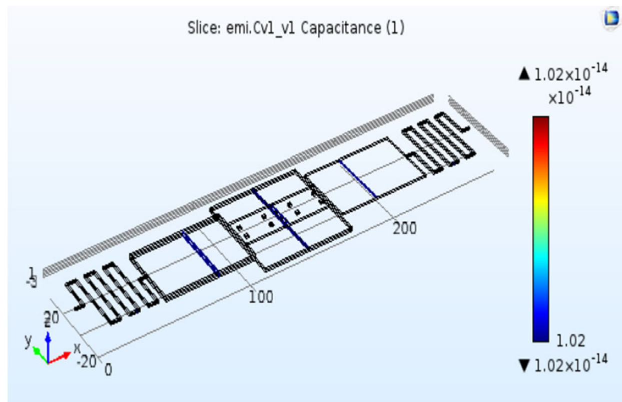

Fig. 22 Upstate Capacitance of the serpentine step switch

generated pulls the beam down so that it makes a contact with the CPW line. When the voltage is applied between the beam and the dielectric layer capacitance can be induced and they can act as a parallel plate capacitor. The insertion loss and isolation of the switch are determined and examined using the Ansys HFSS software (Figs. 23, 24, 25, 26, 27, 28, 29).

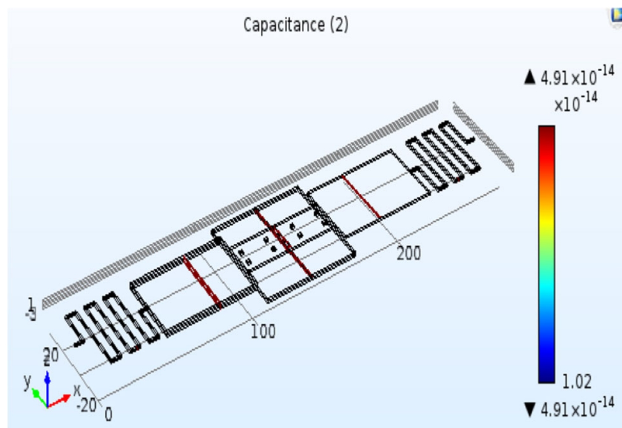

Fig. 23 Downstate capacitance of serpentine step switch

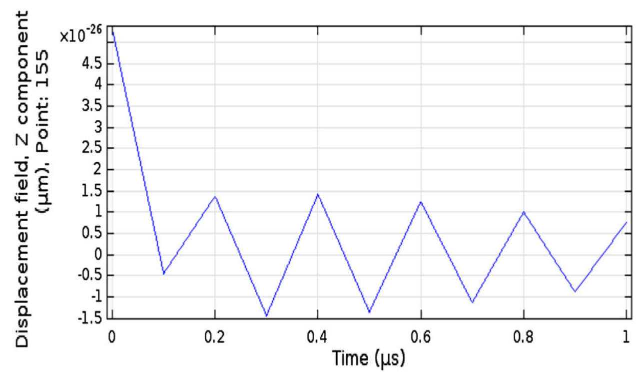

Fig. 24 Switching time of serpentine step switch

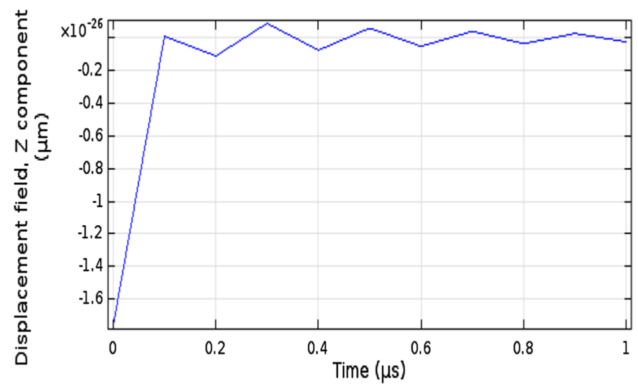

Fig. 25 Switching time analysis of plus meander step switch

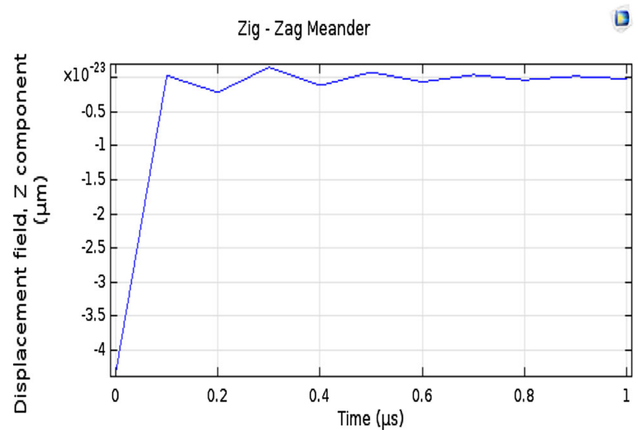

Fig. 26 Switching time of zig-zag meander switch

Return loss (S11 parameter) is also one of the important characteristics of a device to determine the level of impedance matching to make sure the signal is transmitted efficiently. The Insertion loss (S12) of the switches occurs due to the material properties of the substrate. The high dielectric constant will reduce the insertion losses (Verma and Singh 2013).

The isolation loss (S21) is caused when beam touches the signal line and is measured when device is in off-state

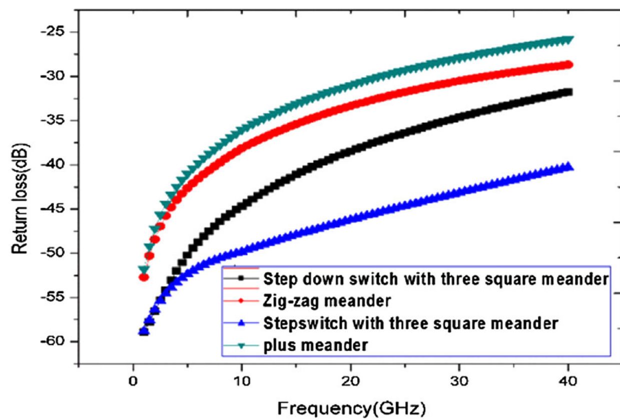

Fig. 27 Return loss of proposed switches

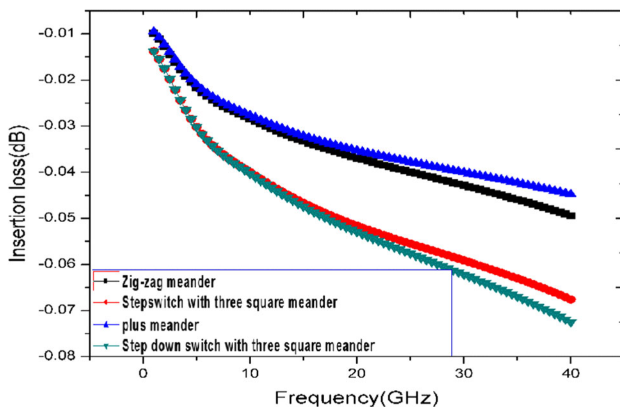

Fig. 28 Insertion losses of proposed switches

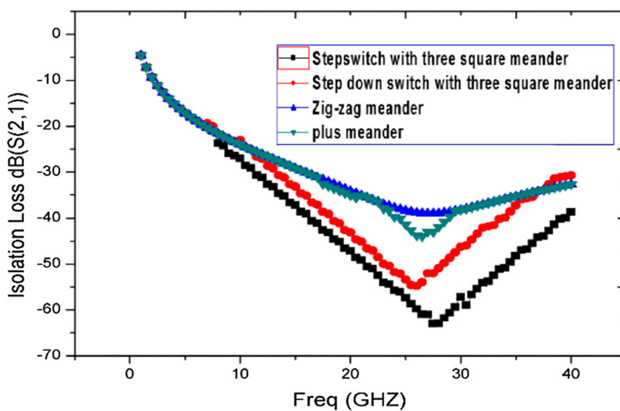

Fig. 29 Isolation losses of proposed switches

(Lee et al. 2015). This isolation (S21) shows how efficiently the device can avoid the leakages currents.

The stepdown structure with three square meanders is showing a low return loss (S11) of − 25 dB and low insertion loss of − 0.07 dB at 40 GHz and a high isolation of − 64 dB at 28 GHz.

4 Conclusion

In this paper, a comparative analysis of two types of switches with three meandering technique have been proposed and analysed. The switches are analytically modelled and validated using FEM simulations. Among the six different types of structures the step structure using serpentine meanders has a very low pull-in voltage of 1.2 V. The serpentine step structure design is processed for different simulation to obtain its performance. The serpentine switch switch exhibits high capacitance ratio of 48 with upstate of 1.02 fF and downstate of 49.1 fF. The fast transition time of 0.2 µs is obtained to change its state from ON to OFF. The switch also exhibits good RF performance characteristics and hysteresis of the switch is studied to understand its behaviour during operation. The proposed switch also exhibits good RF performance characteristics with an insertion loss below − 0.07 dB and return loss below − 60 dB over the frequency range of 1–40 GHz. At 28 GHz a high isolation of − 68 dB is exhibited.

Acknowledgements The Authors would like to thank to NMDC supported by NPMASS, National Institute of Technology, Silchar for providing the necessary computational tools.

References

Angira M, Rangra K (2015) Design and investigation of a low insertion loss, broadband, enhanced self and hold down power RF-MEMS switch. Microsyst Technol 21(6):1173–1178

Bachman M, Yang Z, Minfeng W, Li G (2012) High-power magnetically actuated microswitches fabricated in laminates. IEEE Electron Device Lett 33(9):1309–1311

Balaraman D, Bhattacharya SK, Ayazi F, Papapolymerou J (2012) Low-cost low actuation voltage copper RF MEMS switches. IEEE Microw Theory Tech Symp 2:1225–1228

Chakraborty A, Gupta B, Sarkar BK (2014) Design, fabrication and characterization of miniature RF MEMS switched capacitor based phase shifter. J Microelectron 45:1093–1102

Fedder GK (1994) Simulation of micro-electro-mechanical systems. Ph.D. Dissertation, Electrical Engineering and Computer Science, University of California at Berkeley, USA

Guha K, Kumar M, Parmar A, Baishya S (2016) Performance analysis of RF MEMS capacitive switch with non-uniform meandering technique. Microsyst Technol 22(11):2633–2640

He X, Lv Z, Liu B, Li Z (2011) Electro thermally actuated RF MEMS capacitive switch with automatic layer deposited (ALD) dielectrics. In: 16th international conference on solid-state sensors, actuators and microsystems conference, (RANDUCERS), pp 2470–2473

Jaspreet MH et al (2014) Methods for the minimization of actuation voltage in MEMS. Int J Eng Res Appl 4(3):23–27

Katehi LPB, Harvey JF, Brown E (2002) MEMS and Si micromachined circuits for high frequency applications. IEEE Trans Microw Theory Tech 50(3):858–866

Kumar PA, Sravani KG, Sailaja BVS, Vineetha KV, Guha K, Rao KS (2018) Performance analysis of series: shunt configuration-based RF MEMS switch for satellite communication applications. Microsyst Technol. https://doi.org/10.1007/s00542-018-3907-1

Lee J, Yang WS, Kang S, Choi CA (2015) Design and parameter extraction based small-signal modelling of a novel centre-anchor MEMS series switch. In: Proceedings of the 34th European Microwave Conference, Amsterdam, The Netherlands, pp 1433–1436

Marcelli R, Lucibello A, De Angelis G, Proietti E, Comastri D (2010) Mechanical modelling of capacitive RF MEMS shunt switches. Microsyst Technol 16:1057–1064

Molaei S, Ganji BA (2017) Design and simulation of a novel RF MEMS shunt capacitive switch with low actuation voltage and high isolation. Microsyst Technol 23(6):1907–1912

Öjefors E (2004) Micromachined antennas for integration with silicon based active devices. Uppsala University, Uppsala

Papapolymerou I, Drayton RF (1998) Micro machined patch antennas. IEEE Trans Antennas Propag 46(2):275–283

Ramli N, Sidek O (2012) Reducing an actuation voltage of RF MEMS capacitive switch through three electrodes topology using architect conventorware. J Eng Technol 2(2):46–51

Rao KS, Sravani KG (2018) Design and performance analysis of uniform meander structured RF MEMS capacitive shunt switch along with perforations. Microsyst Technol 24(2):901–908

Rebeiz GM (2003) RF MEMS: theory, design and technology, 3rd edn. Wiley, Hoboken

Roark RJ, Young WC (1989) Formulas for stress and strain, 6th edn. McGraw-Hill, New York

Sharma A, Shah A, Bharti R (2015) Design and simulation of low actuation voltage perforated shunt RF MEMS switch. Int J Eng Tech Res 3(6):236–242

Sravani KG, Rao KS (2018) Analysis of RFMEMS Shunt capacitive switch with uniform and non uniform meanders. Microsyst Technol 24(2):1309–1315

Verma P, Singh S (2013) Design and simulation of RF MEMS capacitive type shunt switch and its major applications. J Electr Commun Eng 4(5):60–68

Publisher's Note Springer Nature remains neutral with regard to jurisdictional claims in published maps and institutional affiliations.